NASA Contractor Report 191068

Lightweight Solar Concentrator Structures, Phase II

Brian E. Williams and Richard B. Kaplan
Ultramet
Pacomia, California

February 1993

Prepared for
Lewis Research Center
Under Contract NAS3–25418

National Aeronautics and
Space Administration

TABLE OF CONTENTS

LIGHTWEIGHT SOLAR CONCENTRATOR STRUCTURES, PHASE II

Brian E. Williams and Richard B. Kaplan
Ultramet
Pacoima, California 91331

SUMMARY

This report summarizes the results of the program conducted by Ultramet under SBIR Phase II Contract NAS 3–25418. The objective of this program was to develop lightweight materials and processes for advanced high accuracy Space Solar Concentrators using rigidized foam for the substrate structure with an integral optical surface.

In particular, this program addressed the development, production, and evaluation of 6-in. diameter by 0.5-in. thick experimental concentrator structures with target properties of 72-in. radius of curvature, areal density less than 0.10 g/cm^2, surface roughness of less than 50 Å RMS, and surface slope error less than 1.0 mrad. By comparison, existing technology for this application yields a slope error of 2.0 mrad at an areal density of greater than 0.5 g/cm^2.

The structural support for the optical surface is a lightweight (0.12 g/cm^3), open-cell ceramic-infiltrated reticulated vitreous carbon (RVC) foam manufactured at Ultramet by converting a commercially available polymer foam to vitreous carbon through a resin infiltration and pyrolysis cycle. The entire ligament structure of the RVC foam was then uniformly coated with a co-deposit of hafnium carbide (HfC) and silicon carbide (SiC) by chemical vapor infiltration (CVI). This material had previously demonstrated excellent high temperature oxidation resistance as well as a high structural stiffness.

Three candidate concentrator faceplate materials for the optical surface were evaluated for use with the ceramic foam structural support. These were optical quartz (fused silica), a high temperature epoxy (polymer), and silicon carbide, which was applied by chemical vapor deposition (CVD).

A quartz faceplate, with HfC/SiC-foam structure (6-in. diameter by 0.5-in thick by 72-in. radius of curvature) was successfully fabricated exceeding the optical specifications, exhibiting a surface slope error of 0.38 mrad with a surface roughness of less than 20 Å RMS. The experimental panel retained these properties during extensive thermal cycling, successfully withstanding three cycles from ambient temperature to −193 °C and back to ambient, 200 cycles from ambient temperature to 120 °C and back to ambient, and 200 cycles from 0 to 120 °C and back to 0 °C. Interferogram measurements were taken after every 20 cycles. The areal density of the final structure was 0.35 g/cm^2, not meeting the desired value of 0.10 g/cm^2 but representing a significant reduction from the 0.50 to 0.60 g/cm^2 value of state-of-the-art lightweight solar concentrators. In addition, a preliminary study of scaleup to 1-m diameter panels was performed. Follow-on work was outlined and directed at optimizing areal density and meeting scaleup requirements.

The quartz faceplate was downselected for fabrication due to its high degree of thermal stability, polish-ability, and compatibility with the ceramic foam support. The polymeric and CVD SiC materials were eliminated due to problems associated with distortion and processing, respectively.

1.0. INTRODUCTION

Solar dynamic power is being evaluated by NASA for electric power production in future applications. A recent NASA-funded system definition study identified nearly 100 missions in the 1992-2010 time frame requiring power systems of 3 kW, and many that will use over 15 kW (ref. 1). A study conducted by the Civil Missions Advisory Group defined future missions to include the Space Station, Earth-orbiting satellites, and asteroid exploration. All of these missions could be accomplished with advanced solar dynamic (ASD) power systems. They offer the potential for efficient, lightweight, survivable, relatively compact, long-lived space power systems capable of a wide range of power levels (3 to 300 kW) and a wide variety of orbits.

The key components of ASD power systems are the solar concentrator, heat receiver with thermal energy storage, heat engine and the radiator. This program focused on concepts for advanced concentrators for ASD systems.

The objective of NASA's Advanced Space Solar Concentrator (ASSC) program is to develop technology for accurate high efficiency, lightweight, long-lived, scaleable, and auto-deployable advanced concentrators (ref. 2). The specific goals are:

Concentration ratio:	2000 to 5000
Collection efficiency:	approximately 95 percent
Weight (areal density):	0.098 g/cm^2
Service life:	up to 15 years

To achieve high concentration ratios, the geometric contour of the concentrator must conform very accurately to that of the ideal parabolic surface. High accuracy is achievable if the slope errors on the concentrator surface are less than 1.0 mrad by comparison. Current concentrator technology yields slope errors of 2.0 to 4.0 mrad. The overall concentrator mass must be reduced from the current technology level of 4.9 to 1.0 kg/m^2 or less, for advanced systems. Current concentrator technology incorporates the use of aluminum honeycomb that is bonded to formed and pre-cut aluminum sheets in the fabrication of a concentrator panel. The approach in this program was to investigate the use of ceramic foam for structural rigidity in lieu of aluminum honeycomb. An optical surface was then applied to the ceramic foam. A number of candidate materials were evaluated. Experimental panels were fabricated and tested. The test results demonstrated that high accuracy panels could be fabricated with this approach and that the specific weight could be reduced below the current state of the art.

2.0. CONCENTRATOR DESIGN CONSIDERATIONS

2.1. Concentrator Optical Requirements

Concentrator panels for space solar concentrators must meet requirements for surface quality, dimensional stability, low mass per unit area, and low cost. The optical surface, quality and dimensional stability requirements for concentrator panels are driven by the system requirements.

To achieve high operating temperatures, the solar flux intercepted by the concentrator must be concentrated onto a small receiving aperture of the solar heat receiver. The concentration ratio is defined as the ratio of these areas. This ratio must be over 2000 for the higher efficiency, solar dynamic power systems. Performance requirements for a 50-ft diameter system are summarized in table I (ref. 3). The concentration ratio is approximately 2000, with a receiver aperture diameter of approximately 1 ft.

A perfect image of the Sun's disk subtends approximately 0.53°. The image diameter is twice the focal length multiplied by the tangent of 0.53/2°. This image diameter approximately equals the 1-ft receiver aperture diameter for a perfect solar collector mirror with a 100-ft focal length. Concentrator surface tolerances and alignment tolerances spread the sunlight beyond the perfect image, however; the solar concentrator focal length must therefore be shorter than 100 ft. Table I describes requirements for a 50-ft diameter concentrator with a 25-ft focal length.

A surface slope error budget can be calculated for this concentrator, as shown in table II (ref. 3). The concentrator focuses 95 percent of the incident solar energy to a 1-ft diameter receiver aperture. The units of the leftmost column are arc-minutes (1 arcmin = 1/60° = 0.29 mrad). The columns to the right show the slope error contribution to the blur diameter at the receiver, in inches. Surface slope errors were budgeted so that the total blur contribution from misalignment, segment slope errors, etc., is smaller than the 1-ft receiver aperture diameter. The segment slope errors budgeted for the concentrator are approximately 1.0 mrad. This is a manufacturing specification for the ASD concentrator panels.

Specular reflectance of aluminum in the visible range (0.2 to 2.0 μm) should be at least 88 percent (ref. 3). Lower reflectance should require greater concentrator area to maintain the same power output. This reflectivity includes the effects of the aluminum/SiO_x reflective/protective films and scatter due to surface microhardness. The total integrated scatter from specular reflection is proportional to the square of the RMS surface microroughness. Figure 1 shows the graphical relation between required concentrator area and surface microroughness (ref. 3). The surface roughness of low-scatter optical telescopes is less than 25 Å RMS, as indicated by the markers for the Advanced X-ray Astronomy Facility (AXAF) and the Hubble Space Telescope (HST). Surface roughness of less than 50 Å RMS is chosen as a manufacturing specification.

2.2. Concentrator Panel Substrates

Candidate substrate materials for lightweight concentrator panels include glass, aluminum, composites such as graphite/polymers, foamed aluminum core structures, and foamed silicon carbide structures. Questions of suitability remain to be answered for each of these candidates, including:

(1) Fragility of ultralightweight glass panels (less than 20 kg/m^2) with regard to deployment or assembly.

(2) Long-term dimensional stability of graphite/polymer composites when exposed to moisture and high-energy radiation in space.

(3) Possible contamination effects caused by outgassing of polymer composites (postlaunch and space shuttle or Space Station environments).

(4) Problems associated with aluminum honeycomb sandwich panels: i.e., the effects of venting during ascent; of anisotropy during manufacturing and maintenance/control; and of the high expansion coefficient of aluminum when there is a great discrepancy between the manufacturing and operating temperatures of the concentrator; also, potential coefficient of thermal expansion (CTE) mismatch between the panels and the support truss.

(5) Survivability with regard to micrometeorites, atomic oxygen in Low Earth Orbit and orbital debris impacts on the panels during their lifetime.

2.3. Environment

Temperature swings for the solar concentrator on orbit may range from −240 to 120 °C (ref. 3). The concentrator panels must meet the dimensional stability requirements over this temperature range. Interferograms taken at room temperature and during cryogenic cooling are a sensitive tool for evaluating changes in dimensional stability.

The concentrator will be subject to chemical attack by whatever active chemical species are present in orbit; these will be primarily atomic oxygen (AO). Surface degradation due to chemical attack has been observed on several shuttle missions. Materials studies included silver, copper, nickel, magnesium, lead, tungsten, molybdenum, gold, chromium, aluminum, platinum, and palladium. Silver was shown to be particularly susceptible to AO and exhibited significant changes in surface morphology, including flaking and degradation of optical and electrical properties (ref. 4). Optical properties are generally most drastically affected by atomic oxygen. Although metallic materials such as aluminum develop Angstrom-level protection surface oxide layers, their optical properties are negatively affected as well. An additional, highly stable transparent film, such as SiO_x must also be applied in order to ensure maximum protection against AO and handling.

Electromagnetic and charged particle radiation is a further area of concern. Although there are many sources of electromagnetic radiation in space, that emitted by the Sun is predominant within the solar system. The total radiation intensity from the Sun at Earth's orbit amounts to about 1.4 kW/m^2. Although the ultraviolet (UV) component accounts for only 9 percent of the total radiation, it has the greatest effect on materials (ref. 5). Metals either reflect or absorb UV without damage within 0.1 μm of the surface. Nonconductive materials, however, can suffer severe and irreversible damage from solar UV.

Additionally, entrained gases in foam materials present both short- and long-term problems in space applications. The sudden depressurization during ascent can create a strain on the foam that may not be reversible once the internal pressure is relieved by leakage. The escape of gases from the labyrinth will continue for long periods and contributes to outgassing effects, including surface contamination of adjacent components. The foam must either be well-sealed or filled with noncondensible, noncorrosive gases. The effect of micrometeorites on sealed foam must also be taken into consideration.

3.0. EXPERIMENTAL APPROACH

For this Phase II program, Ultramet proposed to infiltrate a low-density reticulated vitreous carbon (RVC) foam, fabricated in-house, with a refractory ceramic via chemical vapor infiltration (CVI), completely coating each foam ligament. Following the infiltration procedure, the initial carbon structure would be removed by oxidation, leaving a free-standing, high-stiffness, chemically stable ceramic foam. This structure would then be utilized as a substrate for a high-quality optical surface, which could be bonded to the foam without substantially increasing the areal density.

The composite concentrator fabrication process involved optimizing the strength-to-weight ratio and thermal stability in oxygen of the ceramic foam substrate and investigating concentrator faceplate materials. The primary candidate faceplate materials investigated were optical quartz, a high temperature epoxy (polymer), and CVD silicon carbide (SiC). The latter was deposited onto the ceramic foam substrate and then polished, while the others were first machined to a mirror surface prior to being bonded to the substrate.

3.1. Ceramic Foam Substrate Fabrication

3.1.1. Carbon foam.—The substrate for ceramic infiltration was carbon foam, with a porosity of 80 pores per inch (ppi). This material is a reticulated open-cell foam composed solely of vitreous carbon, a glasslike carbon that combines some of the properties of glass with those of normal industrial carbon. It has an exceptionally high void volume (97 percent) and a high surface area, combined with self-supporting rigidity. The carbon foam structure acts only as a locator for deposition; its contribution to the overall strength of the final infiltrated structure is minimal.

Carbon foam is very lightweight, with a density of 0.07 g/cm^3, and has a relatively uniform pore distribution. Table III shows the physical properties of typical 65-ppi carbon foam, manufactured at Ultramet from a polymer foam precursor impregnated with furfural-phenolic resins. While not specifically addressed in this program, the production flexibility afforded by in-house fabrication of the carbon substrate allows for the manipulation of both cell size and geometry, as well as integral inclusion of the foam into composite sandwich structures.

The carbon foam substrates are, by their porous nature, poor thermal conductors and as such cannot be heated directly by induction (a standard substrate heating technique for CVD/CVI). Instead, a graphite hot-wall furnace is used to heat the porous substrate prior to infiltration. In this configuration (which is set up within the overall reaction chamber), the graphite furnace is heated by induction, which in turn heats the foam substrate by radiation via the graphite foil and carbon block placed above and beneath the foam, respectively. The plating gases are forced through the foam by means of a pressure gradient induced by a vacuum system. On reaching the heated foam substrate, the plating gases react to deposit the desired material on the foam ligaments, resulting in a uniform deposition (infiltration) through the foam.

3.1.2. Ultra2000 (Hfc/SiC) infiltration.—Ultra2000, based on the hafnium carbide/silicon carbide (HfC/SiC) system, was chosen as the coating material for the carbon foam due to its excellent oxidation resistance and high stiffness. The coating, originally developed by Ultramet under an SBIR Phase II program for the Air Force, is a layered structure of SiC and an HfC-SiC mixture, co-deposited by an alternating-pulse process. Both HfC and SiC have very good high temperature strength.

HfC and SiC are deposited by the following reactions respectively, using the CVD/CVI reactor shown schematically in figure 2:

$$HfCl_4 + CH_4 \rightarrow HfC + 4HCl \quad (1)$$

$$CH_3SiCl_3 \rightarrow SiC + 3HCl \quad (2)$$

The hafnium source material, hafnium tetrachloride ($HfCl_4$) gas, is generated in situ by reacting high-purity hafnium metal chips in a controlled chlorine stream. The other HfC reactant gas, methane (CH_4), is fed directly into the reaction chamber. The gases pass over the foam substrate, which has been heated to deposition temperature as described previously. At the hot substrate surface, the gases react according to reaction (1), forming HfC (deposited on the substrate) and HCl gas (exhausted from the system).

The SiC precursor material, methyltrichlorosilane (CH_3SiCl_3, or MTS) liquid, is bubbled directly into the reaction chamber, where it passes over the heated substrate surface. The MTS thermally decomposes according to reaction (2), forming SiC (deposited on the substrate) and HCl gas (exhausted from the system).

The technique by which the Ultra2000 system is deposited offers the additional advantage of acting as its own grain refiner, promoting continuous heterogeneous nucleation. The result is a 10 to 50 nm grain

size and the tremendous increase in strength concomitant with such a fine grain size. Coatings are uniform and adherent. The microhardness of the coatings is very high, averaging 3450 kg/mm^2.

The Ultra2000 system, developed for the oxidation protection of carbon-carbon composites, has demonstrated such protection to 1800 °C for extended periods (hours) and to 1930 °C for shorter periods, thus substantially raising the effective upper temperature limit for carbon. Additional testing of Ultra2000 and CVD SiC materials to much higher temperatures has also indicated their excellent ablation resistance up to 2730 °C. The combination of the ultrafine microstructure and layered structure provides drastic increases in fracture toughness (two to four times), modulus (up to six times for porous substrates), and strength (two to three times) when compared to CVD SiC materials.

The mechanical properties of both "bare" carbon and Ultra2000-infiltrated foams were tested by compression between parallel plates mounted on an in-house Instron universal tester, with the results shown in table IV. This type of test is sometimes referred to as an indentation test, because the outer ligaments of the foam are the primary indentation sites for failure. Another type of test involves the encapsulation of the outer ligaments in a polymeric material, in order to better distribute the applied load. The latter type of test generally yields strength values more than three times greater than those obtained from the type of test conducted by Ultramet. Both tests are important, with the choice being strongly dependent upon the expected end use of the tested material; both are valuable as a means of comparing different foams tested simultaneously.

Following the CVI process, the Ultra2000-coated carbon foams were oxidized to remove the initial carbon structure and prevent any subsequent outgassing resulting from carbon oxidation. After oxidation, each Ultra2000 foam substrate (6-in. diameter by 0.5-in. thick) was machined to a 72-in. concave radius of curvature on one surface, in order to accommodate the mirror faceplates. The foam substrates were extremely fragile, and required special tooling to hold the substrate securely during processing. The concave curvature was generated using cast-iron tooling for coarse grinding and a hand grinder at 60 rpm for fine grinding, with either SiC abrasive in a water lubricant or diamond abrasive in an oil lubricant.

3.2. Faceplace Investigation

The materials selection process for the faceplate optical surface was based primarily on the following requirements:

(1) Thermal stability when cycled between −240 and 120 °C
(2) High degree of machinability (optical machining)
(3) Compatibility with stiffened ceramic foam substrates
(4) Scaleability to 1-m diameter panels

Three materials were identified as potentially meeting these criteria: optical quartz, a high temperature epoxy, and CVD SiC. The latter has previously been used effectively as a polishable mirror surface, when deposited on graphite substrates.

Polymer-derived ceramic coatings that could be polished to mirror surfaces were also investigated. These consisted of SiC, derived from Union Carbide Y–12044 vinyllic polysilane, and SiO_2, derived from International Applied Concepts VIE 4BP materials. Both of these materials failed to produce crack-free coatings, due to their high volatile contents that evolved during the curing process. They did show promise as oxidation-resistant coatings, however, as the cracks could be controlled near the surface without permeation through the entire layer.

Additional experiments were conducted involving the application of plain-weave Nicalon (SiC) fabric and porous felt materials to the surface of the ceramic foam, in an attempt to provide a nonporous surface onto which a mirror coating could be applied. These experiments were also unsuccessful, however, as the porosity and surface irregularities contained in these materials could not be sufficiently reduced to meet the desired optical properties. In addition, bonding these materials to the foam surface led to substantial weight increases.

The faceplate materials that were effectively applied to ceramic foam substrates (quartz, epoxy, SiC) were later coated with a thin Al/SiO layer by physical vapor deposition (evaporation) to provide a reflective, oxidation-resistant mirror surface, although this caused a slight increase in the surface slope error.

3.2.1. Quartz faceplates.—The optical quartz (fused silica) faceplates were ground and polished from rough pre-curved quartz blanks, 6-in. diameter by 0.125-in. thick with a 72-in. radius of curvature on each side (concave/convex). The blanks were ground to approximately 0.060 in. thick using a curved cast-iron lap on the concave face with 220 grit SiC in a water lubricant, followed by 25- and then 9-μm aluminum oxide grit. Conventional pitch polishing followed, using cerium oxide polishing compound and a single-spindle polisher with a water lubricant, to obtain the specified curvature, slope error, and surface roughness (72 in., 1.0 mrad, and less than 50 Å RMS, respectively).

All quartz faceplates met or exceeded specifications, whether or not they were ultimately bonded to a ceramic foam substrate. The final radius of curvature of these faceplates was determined, by measuring the focus of a helium-neon laser, to be 72 in. $\pm$5 percent. Surface slope error was determined, using an optical test plate under a monochromatic mercury vapor source, to be less than or equal to 0.50 mrad (averaging approximately 0.33 mrad). Surface roughness was initially determined to be in the range of 15 to 40 Å RMS, substantially confirmed using a surface profiler to be within 20 Å RMS of the initial value (averaging approximately 20 Å RMS).

An aluminum-filled epoxy (Epibond 87803–A/B) was used to bond the polished quartz faceplates to the ground Ultra2000 foam substrates. This epoxy material was chosen for its deflection (heat distortion) temperature of greater than 200 °C, high aluminum content (approximately 20 wt %), and adhesive properties, as well as for oxidation purposes. This material was very effective as an adhesive. It was also investigated as a faceplate material itself but was ineffective, as it was not designed for casting into free-standing shapes.

An initial determination of the thermal and environmental stability of the aluminum-filled epoxy was made through thermogravimetric analysis (TGA). The TGA results obtained for this and two other polymeric materials are shown in figure 3. The TGA experiments involved a 3-hr hold of each cured material in argon at 175 °C, followed by an additional 3 hr in air at the same temperature. Weight loss varied from 0.6 percent for the silicon-based adhesive to 1.6 percent for the vinyllic polysilane. The majority of weight loss occurred during the early stages of the tests, becoming most rapid above 100 °C. This is most likely due to moisture loss, which is supported by the fact that weight loss decreases rapidly once moisture is removed and becomes negligible for the duration of the test. The introduction of air appeared to have little effect on the stability of the materials at 175 °C.

The first quartz-faceplate concentrator specimen that was fabricated had an areal density of 0.55 g/cm^2 and was delivered to NASA Lewis Research Center for evaluation. Subsequent optimization of the three concentrator components (foam, adhesive, faceplate) led to a reduction in areal density to the 0.35 g/cm^2 range (1.6 kg/m^2). Following are the individual contributions of each of the three components of the composite mirror structure to the total weight of the 6-in. diameter by 0.5-thick mirror specimen delivered to NASA Lewis at the conclusion of the program:

Ultra2000 foam substrate:	34 percent (20 g)
Adhesive:	15 percent (9 g)
Quartz faceplate:	51 percent (30 g)
Total weight:	59 g (approximately 0.35 g/cm^2)

This composite mirror, shown in figure 4, was used throughout the testing phase of the program.

3.2.2. Polymeric (epoxy) faceplates.—A high temperature polymeric epoxy, Thermic Engineering type 350 (proprietary), was investigated as a potential mirror faceplate material due to its ease of casting and polishing, low density, good fracture toughness, a high deflection (heat distortion) tem-perature of 230 °C, a shrinkage on curing of only 0.1 percent, and a moisture absorbity of only 0.01 per-cent. Although epoxies are known to be susceptible to reaction with atomic oxygen, it was deemed feasible to later fully encapsulate the faceplate with a protective Al/SiO flash coating.

TGA results for the type 350 epoxy material, as well as a type 450 derivative, are shown in figure 5. Following the curve for the 350 epoxy, the rapid weight loss in 10 min was apparently due to water de-sorption, an explanation supported by the manufacturer's claim of 0.1 percent moisture absorbity. The remaining loss of 0.7 wt % was due to incomplete curing, which was likely affected by the relatively thick (0.2 in.) part that was tested. Most importantly, weight loss became negligible after approximately 250 min, and the material seemed unaffected by the air atmosphere at 175 °C.

This epoxy material was easily cast into 6-in. diameter disks with a 72-in. radius of curvature on each side (concave/convex). The disks were ground to approximately 0.060 in. thick using a curved cast-iron lap on the concave face with 25- and then 9-μm aluminum oxide grit in a water lubricant. Each epoxy faceplate was subjected to 150 °C in air, both before and after machining. The premachining heating was conducted to ensure complete curing, while postmachining heating was performed to evaluate possible distortion. No distortion was noted after either cycle.

The epoxy faceplates polished fairly well using a single-spindle polisher with a water lubricant and various grades of fine grit Al_2O_3, as well as a special pitch mixture with 0.3-μm Al_2O_3 for final surface smoothness. Two polymeric faceplates were successfully fabricated to the desired optical specifications. One cured specimen was effectively polished to a surface roughness of less than 30 Å RMS, with a density of only 1.6 g/cm^3 and a Shore D hardness of 85. This specimen (not bonded to a ceramic foam substrate) was delivered to NASA Lewis for evaluation.

Problems developed, however, with regard to retaining the 72-in. radius of curvature and 1.0-mrad surface slope error. Defects ranged from the polymer faceplate springing out of specification (warping) after being polished and thermally stabilized to the faceplate not bonding to the ceramic foam substrate. Faceplate warping and delamination occurred after attempting to bond the faceplates to the substrates. Apparently, a nonuniform dispersion of the bonding adhesive (the same aluminum-filled epoxy used with the quartz faceplates) contracted nonuniformly upon curing and led to faceplate distortion. The polymer faceplate became more concave during or after the adhesive cure, that is, the faceplate and adhesive pulled away from the foam and separated.

Subsequent attempts to eliminate distortion of the epoxy faceplates during bonding to the ceramic foam substrates were unsuccessful. Although the physical and optical fabrication specifications could be met during grinding and polishing, none of these faceplates could be evaluated during the testing phase, since none remained together as one cohesive composite mirror structure of polymer faceplate, bonding adhesive, and foam substrate.

3.2.3. CVD SiC faceplates.—CVD SiC was chosen as a potential faceplate material for four primary reasons:

(1) SiC coatings can be machined to a high degree of optical quality while remaining relatively lightweight (3.2 g/cm^3).

(2) CVD SiC is extremely inert at temperatures above 1500 °C in air (1 atm) and has high specific strength (4.3×10^3 m).

(3) The CTE of SiC matches well with that of the Ultra2000 foam substrate material.

(4) Recent advances in Ultramet CVD technology have made the fabrication of 1-m diameter mirror surfaces physically and economically feasible.

Flat, 80-ppi Ultra2000 foam disks were used as substrates for the CVD SiC faceplate study, to be followed by deposition on 72-in. radius-of-curvature substrates once the process was optimized.

In order to minimize SiC infiltration into the foam substrate (which would densify the foam, increasing its weight) and provide a uniform surface for SiC deposition, attempts were made to close out the surface porosity of the foam by the application of refractory paste materials, including graphite and SiC.

The graphite paste material (Cotronics 931) pyrolyzes to greater than 99.5 percent graphite, bonds graphite or carbon components for use to 3000 °C, and has a bond strength in excess of 2500 psi. In addition, the material has a CTE of 4.2 ppm/°C, which was considered well suited for use with both the CVD SiC faceplate and the Ultra2000 foam (CTEs of 5.3 and 5.7 ppm/°C, respectively).

CVD SiC is deposited via the hydrogen reduction of methyltrichlorosilane (MTS) at approximately 1200 °C according to reaction (2) described previously:

$$Ch_3SiCl_3 \rightarrow SiC + 3HCl$$

Deposition of SiC onto the surface of Ultra2000 foam substrates was conducted in a CVD reactor similar to that shown schematically in figure 6. A graphite susceptor or "furnace" was used to support and heat the foam substrate.

After consultation with the optical machinist, it was determined that an initial 0.015-in. coating would be required to allow for subsequent machining to the desired optical specifications. Initial experiments failed due to the inability of the ceramic foam material to withstand the stresses generated in the 0.015-in. SiC coating as it cooled from the deposition temperature. The result was a substantial deflection in the composite mirror. To compensate for this, subsequent foam substrates were infiltrated with Ultra2000 to a greater degree, in order to increase stiffness.

Increasing the SiC coating thickness would have been another possible approach to increasing stiffness; however, as coating thickness increases, the quality decreases as the deposit becomes more granular. In addition, internal stresses increase with coating thickness, raising the probability of microcracking.

Although the CTEs of the graphite paste and CVD SiC coating were relatively close, it was hypothesized that the lower CTE of the graphite may have contributed to the microcracking. In order to promote a nearly ideal CTE match, a SiC paste was developed. A 0.015-in. thick SiC coating was then successfully deposited (crack-free) on a 6-in. diameter by 1-in. thick Ultra2000 foam substrate using the

SiC paste (fig. 7); however, this specimen was severely damaged during the subsequent grinding/polishing process, as the mounting fixture failed.

Several SiC faceplates were deposited onto the concave side of 72-in. radius-of-curvature Ultra2000 foam substrates. Many small nodules were randomly scattered over the entire concave SiC surfaces. The faceplates were rough ground using a curved cast-iron lap with 200 grit diamond, such that no surface low points existed. Pre-final grinding was accomplished using 30-μm diamond followed by 9-μm diamond with a curved cast-iron lap. The final curvature and form were obtained with 3-μm diamond and a curved cast-iron lap, and the final smoothness was then achieved with 1-μm diamond and a pitch lap. All SiC machining used an oil lubricant.

The primary fabrication problem during SiC faceplate processing was a tilt in the surface curvature that occurred during the rough (220 grit diamond) grinding. The presence of this tilt was not realized until the grinding process broke through the faceplate to the foam substrate at one side of the mirror assembly. The cause for this tilt may have been the uneven height distribution of the nodules on the surface of the SiC faceplate. Since all of the SiC-faceplate mirror assemblies experienced this problem, none could meet the desired optical specifications or could be evaluated in the testing phase of the program.

However, the remaining areas of the curved surfaces that could be finished, as well as a number of smaller test samples, looked as good as the completed optical quartz faceplate. With a solution to the remaining deposition and fabrication problems, this SiC composite concentrator structure will be extremely promising. This approach clearly warrants further investigation due to the potential of CVD to produce an extremely lightweight, highly polishable SiC surface. The ability to form the concentrator surface while simultaneously bonding it to the foam surface eliminates many of the fabrication problems associated with the quartz-faceplate system, including the need for the polymeric bonding adhesive.

3.3. Testing and Evaluation

3.3.1. Surface roughness determination.—In determining surface roughness, an estimate was first made (based on the experience of the optical polisher) of the surface roughness of three 1-in. diameter polished quartz test pieces. The actual surface roughness was then measured by both optical (WYKO and Chapman Instruments) and mechanical (Sloan Dektak II) surface profilometers.

An example of the surface roughness evaluation process is given by the case of test piece number 2, as all the test pieces had roughnesses of approximately 20 Å RMS or less, and piece number 2 was the worst case. The optical polisher's estimate for the surface roughness of test piece number 2 was 30 to 40 Å RMS. The WYKO and Chapman Instruments optical profilometers gave measurements of 21.1 and 10.0 Å RMS, respectively, at roughly the same position on the sample. The Dektak mechanical profiler gave an estimated value of approximately 50 to 60 Å RMS.

Surface roughness evaluations for all polished components used the worst-case conditions, i.e., the optical polisher's estimate and/or results of the mechanical profiler (when available). Ultimately, the fabricated quartz, polymer, and SiC mirror faceplates could be evaluated by the optical polisher only, as no optical or mechanical surface profilers were available for use at the time the faceplates were available for measurement. Surface roughness estimates for each of the various mirror faceplates were far less than the 50 Å RMS specification.

3.3.2. Optical quality determination (fringe and slope error).—To evaluate the optical quality of a concentrator faceplate, an optical test plate with a 72-in. convex radius of curvature was placed on the

concave curvature of the concentrator faceplate under a mercury vapor light source. When the mirror faceplate and optical test plate are not identical in curvature, an air wedge is formed between the mating surfaces. This produces constructive and destructive bands of light (light and dark fringes, respectively) due to the optical patch length of the air film between the surfaces. A general 2:1 ratio exists between fringe and wavelength.

3.3.3. Concentrator test specimen preparation.—Prior to thermal testing, the quartz faceplate was ground and polished to a 72-in. concave radius of curvature and a maximum slope error of 0.38 mrad (18 fringes per inch), well within the specification of 1.0 mrad. Figure 8 is a sketch depicting the optical quality of the quartz faceplate at this stage, showing the fringe (interference) patterns present. The quartz mirror faceplate was then bonded to the Ultra2000 foam substrate and sent out to be coated with a reflecting aluminum metal film and a protective SiO overcoat.

After coating, the maximum slope error increased from 0.86 to 1.20 mrad (40 to 56 fringes per inch), just exceeding the optical specification, in patterns similar to those depicted in figure 8 but with more fringe in each area. This measurement included an estimate of the very fine optical fringes within the 0.5-in. radius immediately within the circumference of the faceplate. It was very difficult to obtain an accurate fringe count for two reasons. First, the fringe contrast was very poor, as an uncoated test plate on a coated mirror was being utilized and the fringes were thus extremely light, almost blending in with the background. Second, the fringes were so close to each other that the individual fringes often could not be resolved, a problem compounded by their lightness. These numbers were thus estimates only and should be verified with an optical interferometer, especially if future work will be based on any of these results. Attempts to photograph the quartz-faceplate mirror were unsuccessful.

4. RESULTS AND DISCUSSION

4.1. Low Temperature Concentrator Testing

Preliminary testing of the 6-in. diameter by 72-in. radius-of-curvature (0.35 g/cm^2 areal density) quartz-faceplate mirror was conducted at Ultramet to give an indication of the performance of the completed lightweight concentrator system, specifically to evaluate the thermal shock resistance of the composite structure, the compatibility of the foam substrate and concentrator faceplate, and the dimensional stability of the mirror surface, and to determine whether thermal cycling caused any degradation in the optical characteristics of the mirror.

The test involved subjecting the mirror structure to a low temperature environment using the apparatus shown schematically in figure 9. The insulating vessel was filled with approximately 2 in. of liquid nitrogen at −193 °C. The concentrator was then lowered into the vessel and placed on a stand that held the specimen 2 in. above the liquid nitrogen. A lid was then set in place for insulation. In addition to the mirror itself, various other materials were inserted into the chamber for comparison purposes. These included soda-lime glass, Devcon low temperature/high expansion epoxy, and the two epoxy materials that were being investigated for adhesive and faceplate applications.

The samples were left undisturbed for 3 min, after which time most of the liquid nitrogen had evaporated. The lid was then removed and the materials allowed to warm to room temperature while remaining in the open testing vessel, which took about 4 min. Three consecutive cooling/heating cycles were conducted. Although the soda-lime glass nearly shattered during the warming part of the cycle, the quartz faceplate withstood the thermal cycling with no visible damage. The high quality of the optical quartz material (low level of contamination and high strength) likely aided this result. In addition, the

material was acid etched during various stages of the machining and polishing process in order to reduce internal stresses. All three polymer materials tested also withstood the cycling with no apparent damage.

4.2. High Temperature Concentrator Testing

Primary cyclic thermal testing was performed by Ono laboratories (Alta Loma, CA) in two phases:

Phase 1: Cycle sample from ambient temperature to 120 °C a total of 200 times at atmospheric pressure. Conduct interferogram measurements (a means of detecting surface dimensional changes) after every 20 cycles.

Phase 2: Upon successful completion of Phase 1, cycle sample from 0 to 120 °C a total of 200 times at atmospheric pressure. Conduct interferogram measurements after every 20 cycles.

In summary, these tests showed the concentration test panel to be able to withstand thermal cycling over the entire temperature range from −200 to 120 °C without significantly deviating from a surface slope error of 1.0 mrad over a 72-in. radius of curvature and a surface roughness of less than 20 Å RMS. Although the test surface exhibited some movement during the course of thermal cycling, at no time during testing did the composite test panel deviate appreciably from the specified surface slope error or roughness.

4.2.1. Phase 1 thermal testing.—Prior to subjecting the actual composite lightweight test panel assembly to the first phase of thermal cycling tests, a preliminary test was performed on a 4- by 4- by 0.060-in. quartz window bonded to a 6-in. diameter foam core backing. Both the foam and epoxy adhesive were identical to those used in the actual test panel assembly. The test window was cycled from ambient temperature to 120 °C at a heating rate of approximately 22.2 °C/min (40 °F/min) and allowed to stabilize for 6 to 10 min at 120 °C, then was immediately removed from the oven and allowed to cool to ambient for 4 to 6 min, then stabilized for 6 to 10 min at ambient. This cycle was performed a total of 12 times. At the end of the preliminary testing, the quartz window showed no visible (macroscopic) damage from the thermal cycling. It was thus assumed that the actual test panel assembly would survive this heating rate and elevated temperature cycling without catastrophic damage.

The Phase 1 thermal cycle testing was conducted on a composite lightweight panel assembly consisting of a 6-in. diameter quartz faceplate bonded to an Ultra2000 foam substrate. The test consisted of subjecting the panel assembly to thermal cycling from ambient temperature to 120 °C at a heating rate of approximately 22.2 °C/min (40 °F/min) and then cooling the panel assembly back to ambient temperature, for a total of 200 cycles. The panel assembly was allowed to stabilize at 120 °C for at least 4 min, after which it was removed and allowed to cool for 8 to 10 min at which time it was no longer warm to the touch.

After 20 cycles, the optical slope error was measured at ambient temperature in order to evaluate any distortion due to the thermal cycling. The slope error test utilized a mercury vapor light source and a 72-in. convex radius-of-curvature optical test plate. Although the panel surface did move during any given 20-cycle set, the slope error within the central 80 percent of the panel remained below the 1.0-mrad specification for most of the testing. The 0.5-in. radius immediately within the circumference of the panel surface had the greatest slope error, but the exact value is unknown since the fringes could not be counted accurately as described previously. The central 80 percent of the panel (interior to the 0.5-in radius around the circumference) did meet the 1.0-mrad slope error specification for 8 of the 10 sets of 20 cycles. Figure 10 shows the fringe pattern following the last (10th) test set. The two test sets that did not meet

the slope error specification, which occurred in the middle of the 10-set Phase 1 testing and did not repeat, showed average errors of 1.14 and 1.29 mrad (53 and 60 fringes per inch, respectively).

Additional testing was conducted in order to monitor the amount of surface movement during the heating cycle from ambient temperature to 120 °C, during stabilization at temperature, and during cooling from 120 °C back to ambient. A helium-neon laser beam was aimed at approximately the center of the test panel and reflected to a position 156 in. from the surface. The oven door was closed, with the laser beam passing through the window in the oven door and reflecting off the surface to the beam monitoring plane 156 in. from the test panel. The oven was activated and ramped up to 120 °C at approximately 22.2 °C/min (40 °F/min), then the test panel was stabilized at 120 °C for 16 min. The laser beam was stationary throughout this procedure. The oven was then opened and the test panel allowed to cool back to ambient temperature. After 1.5 hr, the oven and test panel assembly were cooled internally to 32 °C; the beam again remained stationary.

The aim point of the laser beam was then moved to a position about 0.5 in. in from the edge of the test panel. The oven was then heated back to 120 °C and again stabilized for 16 min. At this point, the laser beam moved approximately 0.35 cm (0.88 mrad); however, the test panel surface normal actually moves only half the angular error value, or 0.44 mrad. The oven was then opened and the test panel allowed to cool back down to ambient temperature. After 1.5 hr of cooling, the laser beam moved another approximately 0.8 cm (2.02 mrad), with the actual normal movement of the test panel surface thus being 1.01 mrad.

This test, with the laser beam at 0.5 in. in from the edge of the test panel, was then repeated. After heating to 120 °C and stabilizing, the beam movement was 0.5 cm (1.26 mrad), equivalent to a test panel surface normal movement of 0.63 mrad. Beam movement after cooling from 120 °C to ambient temperature and stabilizing was approximately 0.4 cm (1.01 mrad), or a surface normal movement of 0.5 mrad.

Thermal cycling of the quartz test panel assembly thus did not distort the surface or produce any visible effects over its central 80 percent. In the outer 20 percent (0.5 in. in from the edge), however, the surface bent 0.44 to 0.63 mrad in towards its optical axis during heating, and 0.50 to 1.01 mrad away from its optical axis during cooling. This effect on slope and power is to be expected with quartz, and even the worst-case surface movement for this test panel, 1.01 mrad at 0.5 in. in from the circumference, is just barely above the 1.0-mrad specification.

In summary, the quartz faceplate/foam substrate composite lightweight test panel assembly performed reasonably well throughout the Phase 1 thermal testing. Constant, variable test panel face movement was observed throughout the test, but in nearly all cases the slope error remained within the 1.0-mrad specification. The slope error exceeded the specification twice during Phase 1 testing, but these values of 1.14 and 1.29 mrad should not affect the overall performance of a 6-in. diameter test panel. The test panel face movement was found to be in a direction that would cause the focus length to shorten on heating from ambient temperature to 120 °C, which may or may not be a problem depending on the surface area (size) of the concentrator. Due to the surface movement observed, operational environmental testing should be performed on any larger concentrator assemblies of this type because the results obtained with the 6-in. diameter quartz test panel assembly may not necessarily scale linearly with size or guarantee good optical performance.

4.2.2. Phase 2 thermal testing.—The same test panel that underwent Phase 1 thermal cycle testing was also used in the Phase 2 testing. The Phase 2 testing was designed to subject the test panel assembly to a temperature range of 0 to 120 °C, according to the following procedure:

(1) Place test panel assembly in oven at ambient temperature
(2) Heat to 120 °C at heating rate of approximately 22.2 °C/min (40 °F/min)
(3) Stabilize at 120 °C for 4 to 6 min
(4) Remove test panel assembly from oven and allow to cool in ambient temperature air for 8 min
(5) Place test panel assembly in 0 °C freezer and allow to cool for 8 min
(6) Remove test panel assembly from freezer and allow to warm in ambient temperature air for 8 min
(7) Repeat steps 1 to 6, 20 times
(8) Measure surface slope error of test panel at ambient temperature after 20 cycles
(9) Repeat steps 7 and 8 a total of 10 times, or 200 complete cycles and 10 slope error tests

The slope error test utilized the same mercury vapor light source and 72-in. convex radius-of-curvature optical test plate as had been used during the Phase 1 testing. As in Phase 1, the test panel surface moved during any given 20-cycle set in Phase 2 testing, with the slope error remaining within the 1.0-mrad optical specification in 7 of 10 measurements made. In no case did the test panel assembly show any sign of breakage or other macroscopic physical damage.

Figures 11(a) to (d) depict the general fringe (interference) patterns, measured at ambient temperature, of the surface before, during, and after the Phase 2 thermal cycle testing: prior to beginning thermal cycling; after the first set of 20 cycles; after five sets of 20 thermal cycles; and after completing all 200 thermal cycles, respectively.

Two of the three slope error test values that exceeded specifications occurred within the first three sets of 20 cycles, with average errors of 1.1 and 1.3 mrad (52 and 60 fringes per inch, respectively). The third out-of-specification value occurred after the 14th cycle, just barely exceeding the specification with a slope error of 1.04 mrad (48.7 fringes per inch).

In summary, the quartz-faceplate/foam substrate composite lightweight test panel assembly performed very well throughout the Phase 2 thermal testing. Constant, variable face movement was observed from both heating and cooling cycles, but the slope error remained within the 1.0-mrad specification in most cases. The slope error exceeded the specification three times during Phase 2 testing, but these values of 1.04, 1.1, and 1.3 mrad should not affect the overall performance of a 6-in. diameter test panel. As with the Phase 1 testing, due to the surface movement observed, operational environmental testing should be performed on any larger assemblies of this type because the results obtained with the 6-in. diameter quartz test panel assembly may not necessarily scale linearly with size or guarantee good optical performance.

5. CONCLUSIONS AND RECOMMENDATIONS

A quartz-faceplate/Ultra2000 (HfC/SiC) foam composite lightweight concentrator structure was developed in this program, and a 6-in. diameter, 72-in. radius-of-curvature rigid test panel was subsequently fabricated to meet optical specifications consisting of a surface slope error of less than 1.0 mrad and a surface roughness of less than 50 Å RMS. In addition, the test panel retained these properties during extensive thermal cycling, successfully withstanding three cycles from ambient temperature to −193 °C and back to ambient, 200 cycles from ambient temperature to 120 °C and back to ambient, and 200 cycles from 0 to 120 ° and back to 0°.

The areal density of the final quartz/foam structure was reduced to 0.35 g/cm^2, still not meeting the desired value of 0.10 g/cm^2. The factors limiting further reductions to the areal density of this particular composite system include the requirement for the adhesive material used to bond the optical faceplate to

the foam substrate, and the faceplate thickness necessary to survive the polishing process. It should be noted, however, that the 0.35 g/cm^2 areal density achieved in this program represents a significant reduction from the 0.5 to 0.6 g/cm^2 value of state-of-the-art lightweight concentrators with unmatched optical properties.

The CVD SiC faceplate/Ultra2000 foam system has not been optimized and warrants further investigation. This system could simplify the concentrator fabrication process by combining the faceplate fabrication and bonding processes into one step. It is estimated that a SiC/foam composite concentrator may be fabricated to the desired optical specifications at an areal density in the range of 0.2 to 0.3 g/cm^2.

Another potential improvement that should be investigated is the use of vitreous carbon as a concentrator faceplate material. Vitreous carbon is lower in density (1.6 g/cm^3) than either graphite or diamond, and cannot be graphitized. It is also highly corrosion-resistant (i.e., possesses low gas permeability) and is similar to glass in both appearance and fracture properties. Table V shows the high strength and hardness of vitreous carbon in comparison to other forms of carbon. Under internal funding, Ultramet is exploring the fabrication of near-full-density plates of vitreous carbon that are highly polishable. The end use of this material would involve incorporating these thin, dense plates with a highly porous RVC foam support, which could be accomplished as part of the RVC foam fabrication process itself. The potential of this material/process for application to lightweight concentrator structures is considerable, in terms of both improved properties and ease of fabrication, and should be pursued.

A basic study of quartz concentrator scaleup was performed, with the results shown in table VI for the estimated change in mirror fabrication costs with increased concentrator diameter. Although the quartz faceplate and ceramic foam costs are shown to increase at similar rates, in reality the quartz material dominates as the primary cost. For applications requiring lower costs, alternative faceplate materials such as SiC and vitreous carbon show considerable promise.

Finally, Ultramet would like to thank Russell Ono of Ono Laboratories and Lawrence Scheer of Cyto Optics for their assistance in defining testing procedures and integrating the concentrator test panel surfacing process with Ultramet fabrication. In addition, Ultramet extends thanks to Joseph M. Savino and Thaddeus S. Mroz of NASA Lewis Research Center for their continuous interest in this program and their input as the NASA project managers.

REFERENCES

1. Savino, J.M., et al.: Advanced Solar Dynamic Space Power Systems Perspectives, Requirements and Technology Needs. NASA TM–88884, 1987.

2. Savino, J.M.: Personal Communication with J.G. Sheek, Aug. 1987.

3. Krim, M.H.: Application of Replicated Glass Mirrors to Large Segmented Optical Systems—For Space Structures. Large Optics Technology; Proceedings of the Meeting, SPIE Proceedings, Vol. 571, G.M. Sanger, ed., SPIE, Bellingham, WA, 1986, pp. 60–76.

4. Swanson, P.N., et al.: System Concept For a Moderate-Cost Large Deployable Reflector (LDR). Opt. Eng., vol. 25, Sept. 1986, pp. 1045–1054.

5. Fromhold, A.T.: Characterization of Material Surfaces Exposed to Atomic Oxygen on Space Shuttle Flights. 1984 NASA/ASEE Summer Faculty Fellowship Program, NASA CR–171317, 1985, p. 12.

TABLE I.—PERFORMANCE REQUIREMENTS FOR 50-FT DIAMETER SOLAR CONCENTRATOR MIRROR PANEL (ref. 3)

Orbit-average electrical power, kW	320
Output (8 to 10 individual power systems at 35 to 40 kW each)	
Orbital altitudes, inclination, nm (deg)	250 to 270 (28)
Operational readiness	1992 IOC at 80 kW 1995 to 1996 FOC at 320 kW
Collecting area	20 000 to 25 000 ft^2 at 320 kW (depending on cycle efficiency)
Aperture diameter, ft	50 to 60
Focal length (on-axis), ft	25 to 30
Operational life	≥7 years with less than 10 percent output degradation
Total weight/40 kW system, lb	16 000
Packaged volume/40 kW system	15-ft diameter by 28-ft length
Cost/kW hr	As low as possible
Receiver interface	95 percent of reflected energy into receiver aperture

TABLE II.—SURFACE SLOPE ERROR BUDGET FOR 50-FT DIAMETER SOLAR CONCENTRATOR MIRROR PANEL (ref. 3)

[2000:1 Concentration ratio Brayton system.]

	Slope error, RMS	Simple "parabola," f/0.5	Compound		
			f/0.5	f/1	f/2
Solar image	N/A	5.9	5.9	1.8	24.0
Segment alignment					
Initial alignment accuracy	1.6 $\hat{m}$	1.7	1.7	3.4	6.8
Thermal deformations	1.6 $\hat{m}$	1.7	1.7	3.4	6.8
Structural deflections	1.6 $\hat{m}$	1.7	1.7	3.4	6.8
Segment slope errors	5 $\hat{m}$ overall				
Design residual	3 $\hat{m}$	1.7	1.7	2.4	6.8
Fabrication	1 $\hat{m}$	1.2	1.2	2.4	4.8
Quilting/bending	1 $\hat{m}$	1.2	1.2	2.4	4.8
Constraint forces	1 $\hat{m}$	1.2	1.2	2.4	4.8
Secondary mirror					
Slope error	5 $\hat{m}$	N/A	0.7	1.4	2.8
Alignment error	5 $\hat{m}$		0.7	1.4	2.8
Pointing and jitter	0.1° RMS	1.7	1.7	3.4	6.8
Receiver/concentrator alignment	±1 in.	1	1	1	1
		11.3	11.3	21.7	42.0
		Inches 2			

TABLE III.—PROPERTIES OF CARBON FOAM

[ULTRAFOAM$_C$ open-cell carbon foam.]

Typical physical properties	
Micrographic porosity, ppi	58.8
Ash content, wt %, 1000 °C	0.39
Bulk density, g/cm^3	0.042
Ligament density, g/cm^3	1.538
Surface area, m^2/g	1.623
Resistivity, Ω-cm	0.75
Specific heat, cal/g/°C	0.30
Maximum use temperature, °C	in air: 350
	inert: 3500
Thermal expansion, pp/°C	0 to 200 °C: 1.15
	0 to 500 °C: 1.65
	0 to 1000 °C: 1.65
Thermal conductivity, W/m·K	200 °C: 0.085
	300 °C: 0.125
	400 °C: 0.180
	500 °C: 0.252
	650 °C: 0.407
	800 °C: 0.625
	950 °C: 0.882
Compressive strength, kPa, 20 °	625 (10 percent deflection)
	763 (ultimate)
kPa, 1000 °C	391 (10 percent deflection)
	628 (ultimate)
Shear strength, kPa, 20 °C	290
Tensile strength, kPa, 20 °C	810
Flexure strength, kPa, 20 °C	862
Flexure modulus, MPa	58.6

TABLE IV.—COMPRESSIVE STRENGTH OF ULTRAMET RVC AND ULTRA2000 FOAMS

Material, ppi	Density, g/cm^3	Compressive strength		Specific compressive strength, MPA/g/cm^3
		psi	kPa	
Ultramet RVC				
20	0.046	7±2	52±14	1.20±0.3
45	.060	9±1	62±10	1.03±0.17
65	.060	30±10	207±69	3.50±1.2
80	.065	43±6	296±41	4.55±0.63
Ultra2000				
20, 6 percent	0.041	40±7	276±48	1.94±0.39
80, 6 percent	.161	220±30	1517±207	9.42±1.29
80, 12 percent	.353	336±50	2523±345	7.15±0.98
80, 18 percent	.545	473±20	3263±138	5.99±0.25

TABLE V.—PROPERTIES OF CARBON PRODUCTS

Property		Baked carbon	Electrode graphite	Morganite EY9	Vitreous carbon
Apparent density, g/cm^3		1.57	1.55	1.7	1.47
Porosity, percent		200 to 30	20 to 30	17	<0.05
Gas permeability, cm^2/sec		----------	>20	0.015	$<2.5\times10^{-11}$
Transverse strength, $lb/in.^2$	With grain	1100	1000	5800	10 000 to 30 000
	Across grain	800	700	1900	
Compressive strength, $lb/in.^2$	With grain	3800	2900	7400	10 000
	Across grain	-------	-------	3300	
Young's modulus, 10^6 $lb/in.^2$	With grain	1.2	0.6	1.9	3 to 4
	Across grain	-------	-------	0.7	
Electrical resistivity, 10^{-4} Ω·cm	With grain	50	9	19	30 to 80
	Across grain	75	11	39	
Thermal conductivity, cal/cm·sec·°C	With grain	0.017	0.22	0.14	0.01 to 0.02
	Across grain	-------	0.17	0.11	
Thermal expansion, ppm/°C	With grain	-------	2.2	1.8	2.2 (0 to 100 °C)
	Across grain	-------	3.6	4.0	3.2 (100 to 1000 °C)

TABLE VI.—ESTIMATED SCALEUP COSTS[a]

Mirror diameter, in.	Ultra2000 foam (CVI and machining)	Quartz faceplate (includes grinding and polishing)	Bonding (curing)	Total cost
6	$185	$ 565	$135	$ 885
12	341	1 736	290	2 367
20	1245	5 360	472	7 077
24	2312	8 750	550	11 612
30	4445	16 320	720	21 485

[a]Based on fabrication of six pieces.

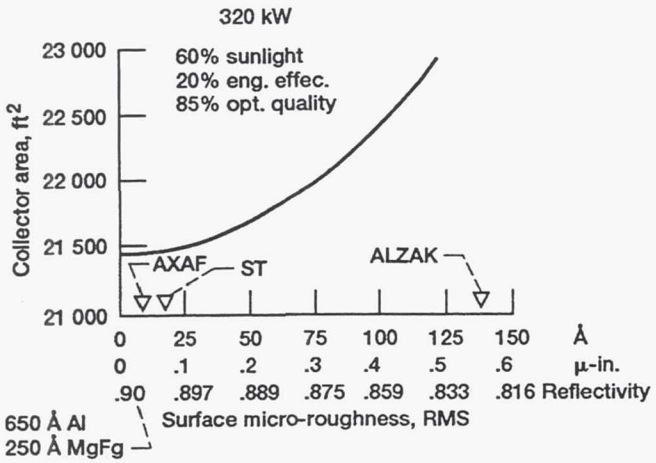

Figure 1.—Effect of surface roughness on required concentrator area [3].

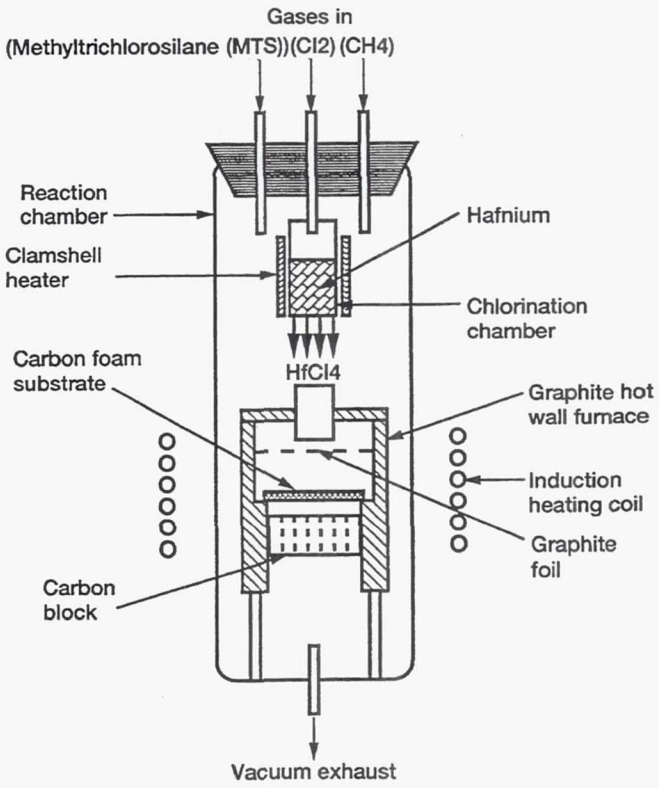

Figure 2.—Schematic of CVD/CVI apparatus deposition/infiltration of Ultra2000 (HfC/SiC) into carbon foam substrate.

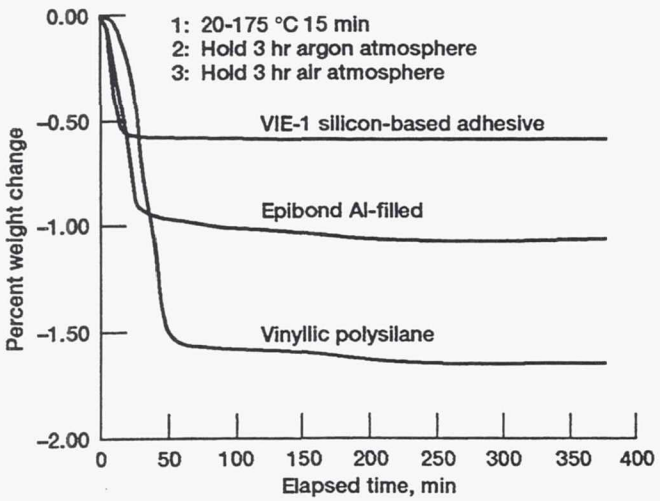

Figure 3.—TGA results for candidate adhesive materials. (Harrop Industries TGA test number HL-3378).

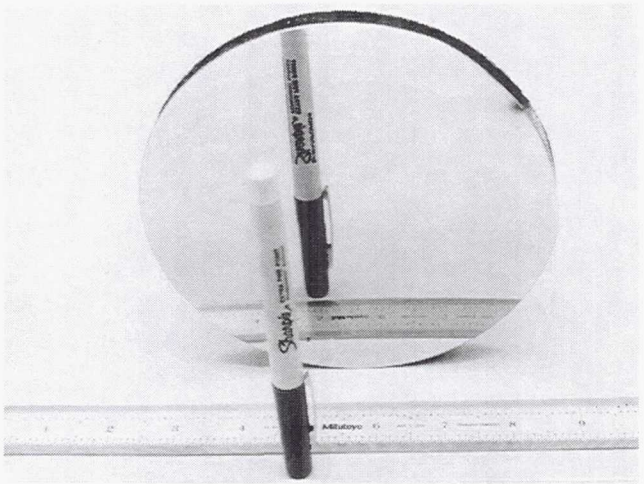

Figure 4.—Completed quartz-faceplate/Ultra2000 (HfC/SiC) foam composite lightweight concentrator structure, with aluminum reflecting film and SiO protective overcoat. Specifications: 6 in. diameter, 72 in. radius of curvature, <50 Å RMS surface roughness, <1.0 mrad surface slope error; 0.060 in. quartz faceplate thickness, 80 ppi foam porosity, 0.35 g/cm^3 areal density.

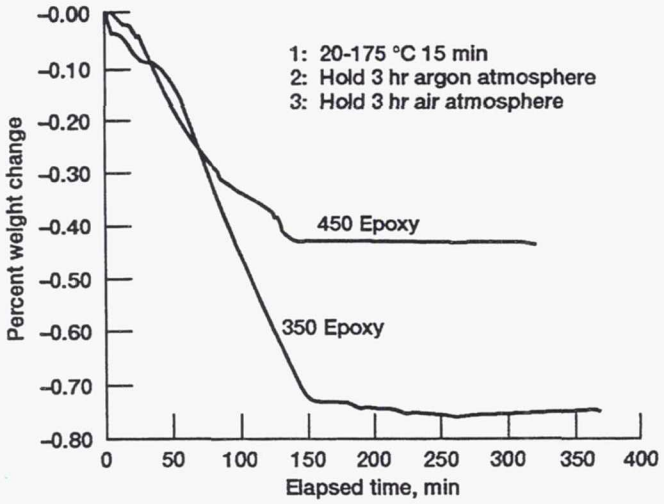

Figure 5.—TGA results for candidate polymer faceplate materials. (Harrop Industries TGA test number HL-3443).

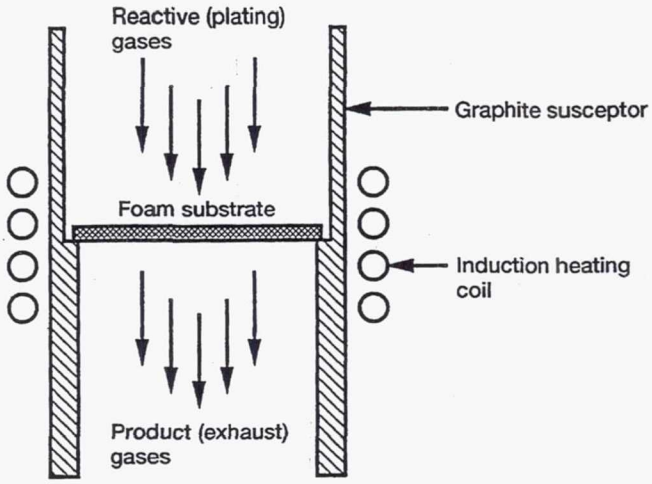

Figure 6.—Schematic of CVD/CVI apparatus for deposition of SiC onto Ultra2000 foam substrate.

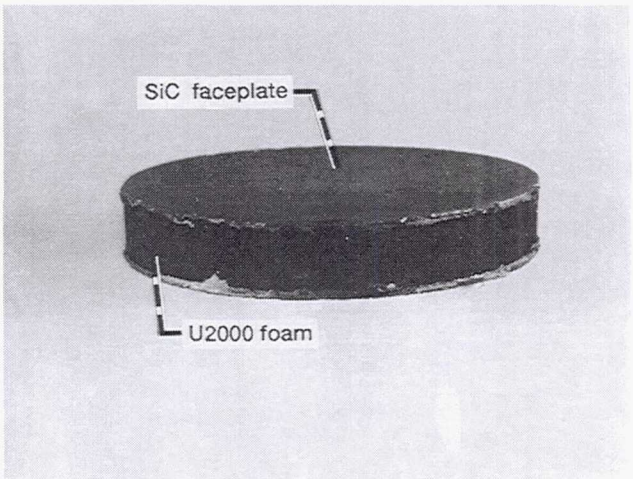

Figure 7.—CVD SiC faceplate/Ultra2000 foam composite lightweight concentrator structure, prior to grinding/polishing/concentrator coating. Specifications: 6 in. diameter, 0.015 in. SiC coating thickness, 80 ppi foam porosity, 0.63 g/cm^3 areal density.

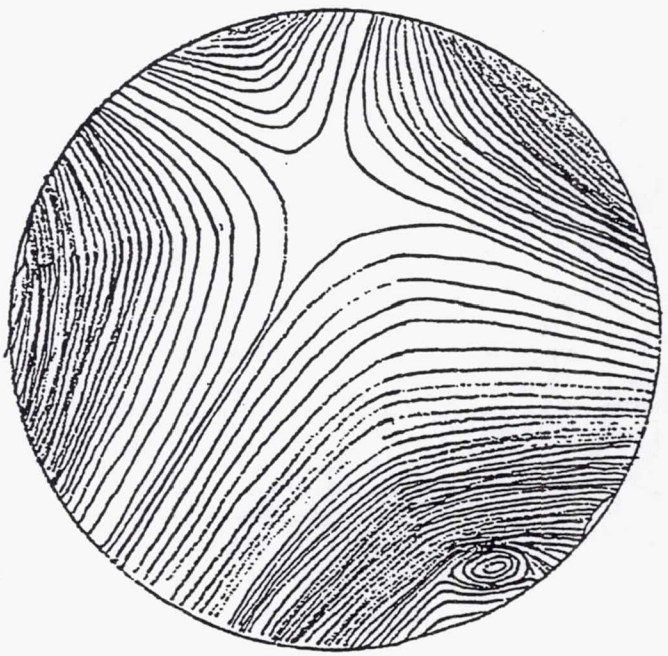

Figure 8.—Depiction of fringe (interference) patterns present in quartz test panel faceplate following grinding and polishing to 72 in. radius of curvature and slope error of <0.38 mrad, prior to bonding to foam substrate and concentrator coating.

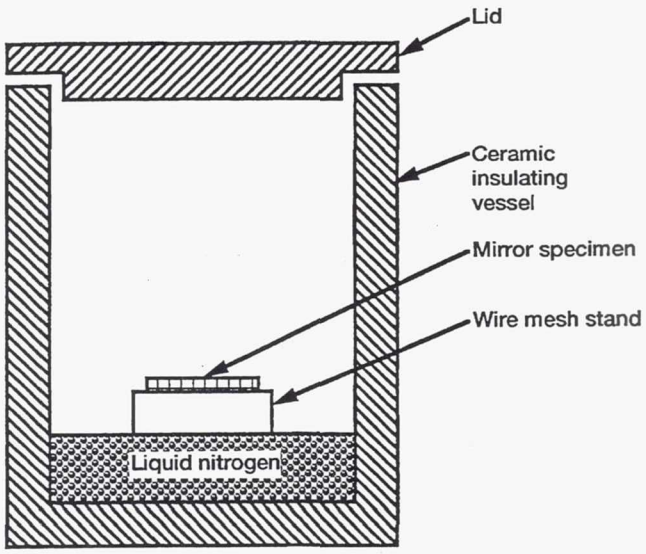

Figure 9.—Schematic of cryogenic testing apparatus for low temperature thermal cycling of a concentrator test panel structure.

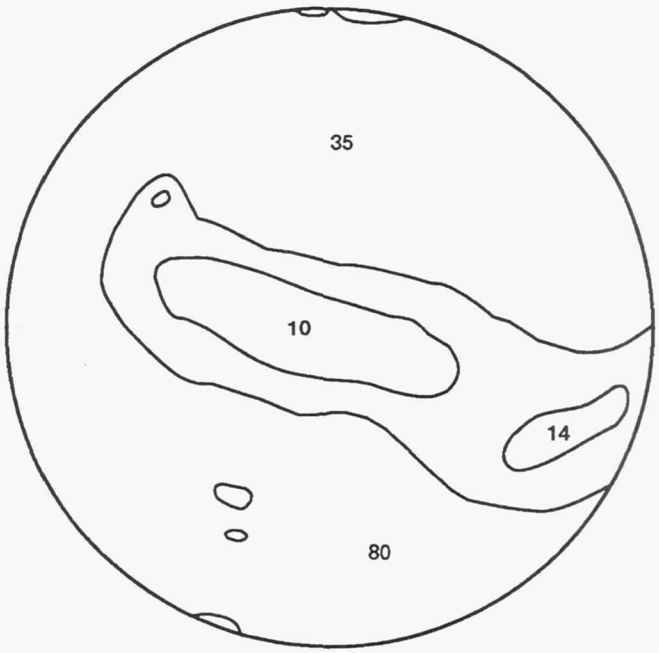

Figure 10.—Quantitative depiction of fringe pattern present in quartz faceplate/foam composite concentrator test panel structure following conclusion of phase 1 thermal testing (200 cycles from ambient temperature to 120 °C and back to ambient).

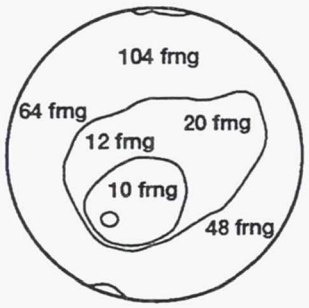

(a) Fringe pattern in quartz-faceplate concentrator test panel; structure before start of phase 2 thermal testing (200 cycles from 0 to 120 °C and back to 0°).

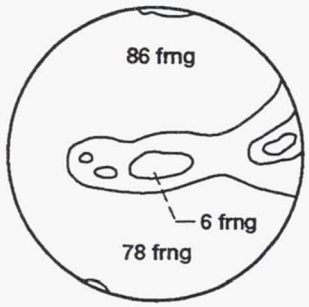

(c) Fringe pattern in quartz-faceplate concentrator test panel structure after five sets of 20 cycles in phase 2 thermal testing.

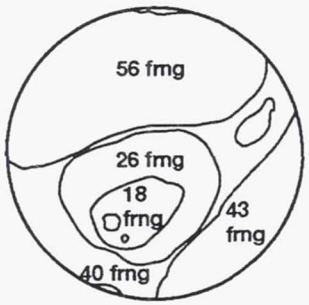

(b) Fringe pattern in quartz-faceplate concentrator test panel after first set of 20 cycles in phase 2 thermal testing.

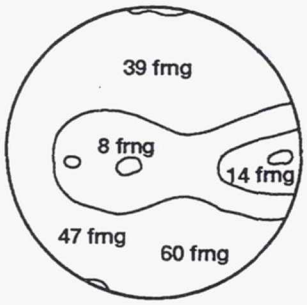

(d) Fringe pattern in quartz-faceplate concentrator test panel structure following conclusion of phase 2 thermal testing (200 cycles from 0 to 120 °C and back to 0°).

Figure 11.—Fringe patterns–thermal cycling test results.

REPORT DOCUMENTATION PAGE

Form Approved
OMB No. 0704-0188

1. AGENCY USE ONLY (*Leave blank*)	2. REPORT DATE	3. REPORT TYPE AND DATES COVERED
	February 1993	Final Contractor Report

4. TITLE AND SUBTITLE

Lightweight Solar Concentrator Structures, Phase II

5. FUNDING NUMBERS

WU–506–41–31
NAS3–25418

6. AUTHOR(S)

Brian E. Williams and Richard B. Kaplan

7. PERFORMING ORGANIZATION NAME(S) AND ADDRESS(ES)

Ultramet,
12173 Montague Street
Pacomia, California

8. PERFORMING ORGANIZATION REPORT NUMBER

E–7576

9. SPONSORING/MONITORING AGENCY NAMES(S) AND ADDRESS(ES)

National Aeronautics and Space Administration
Lewis Research Center
Cleveland, Ohio 44135–3191

10. SPONSORING/MONITORING AGENCY REPORT NUMBER

NASA CR–191068

11. SUPPLEMENTARY NOTES

Project Manager, Thaddeus S. Mroz, Power Technology Division, NASA Lewis Research Center, (216) 433–6168.

12a. DISTRIBUTION/AVAILABILITY STATEMENT

Unclassified - Unlimited
Subject Categories 20, 26, and 27

12b. DISTRIBUTION CODE

13. ABSTRACT ***(Maximum 200 words)***

This report summarizes the results of the program conducted by Ultramet under SBIR Phase II Contract NAS3–25418. The objective of this program was to develop lightweight materials and processes for advanced high accuracy Space Solar Concentrators using rigidized foam for the substrate structure with an integral optical surface.

14. SUBJECT TERMS

Solar concentrator; Lightweight; Foam; Chemical vapor deposition (CVD)

15. NUMBER OF PAGES

24

16. PRICE CODE

A03

17. SECURITY CLASSIFICATION OF REPORT	18. SECURITY CLASSIFICATION OF THIS PAGE	19. SECURITY CLASSIFICATION OF ABSTRACT	20. LIMITATION OF ABSTRACT
Unclassified	Unclassified	Unclassified	